Peertechz

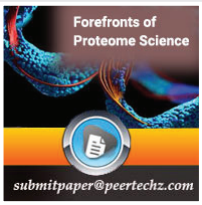

CLINSURG GROUP

Forefronts of Proteome Science

OPEN ACCESS JOURNAL

DOI: https://dx.doi.org/10.17352/fps

Research Article

Photoremoval of Ibuprophenin and Oxytetracycline and some microorganisms from a pharmaceutical wastewater via Ag-Fe_3O_4 nanocomposites

Delia Teresa Sponza* and Rukiye Öztekin

Engineering Faculty, Department of Environmental Engineering, Dokuz Eylül University, Tınaztepe Campus, 35160 Buca/Izmir, Turkey

Received: 14 May, 2024
Accepted: 21 May, 2024
Published: 22 May, 2024

***Corresponding author:** Dr. Delia Teresa Sponza, Professor, Engineering Faculty, Department of Environmental Engineering, Dokuz Eylül University, Tınaztepe Campus, 35160 Buca/Izmir, Turkey,
E-mail: delya.sponza@deu.edu.tr

ORCiD: https://orcid.org/0000-0002-4013-6186

Keywords: Ibuprophene; Oxytetracycline; Field Emission Scanning Electron Microscope (FESEM); Fourier Transform Infrared Spectrophotometer (FTIR); Pharmaceutical wastewater; Silver loaded-magnetic nanoparticles; X-ray diffraction (XRD) analysis

https://www.clinsurggroup.com

Check for updates

Abstract

In İzmir Turkey, a pharmaceutical industry wastewater produces drugs and antibiotics. The removals of these parameters were not sufficient with the conventional activated sludge process. In order to remove these organics some photocatalysts like Fe_3O_4 and FeO were solely used with enhanced magnetic properties. However low photodegradation yields (75% - 77%) were detected for the Ibuprophenin drug and Oxytetracycline antibiotic. Although Ag effectively destroys the pharmaceutical chemicals and the pathogenic microorganisms the low photogenerated carrier-separation efficiency limits its application in water treatment. Therefore, it is practically significant to develop a magnetic material to a couple of Ag with Fe_3O_4 through heterojunctions to separate the nanocomposite magnetically from wastewaters. In order to improve the photocatalytic degradation of Fe_3O_4, Ag was loaded onto a magnetic nanoparticle to develop Ag-Fe_3O_4 nanocomposite under laboratory conditions. On the other hand, the toilet wastewater was mixed with the process wastewater due to the dilution purpose of pollutants in the pharmaceutical wastewater. Due to the high working personnel capacity of the industry (10,000 people) the concentrations of *Salmonella, Pseudomonas*, yeast, fungi, total coliforms, fecal coliforms, and heterotrophic bacteria were found to be high in the raw pharmaceutical industry wastewaters. Therefore, in this study to maximize the removal yields of these pollutants and organisms with Ag-Fe_3O_4 photodegradation the operational conditions were optimized. The effect of increasing Ag-Fe_3O_4 nanocomposite concentrations (0.05 - 6.0 mg/l), pollutant concentrations (10 - 500 mg/l), contacting times (5 - 90 mins), pH levels (4.00 - 10.00), power (10 - 100 W/m^2), on the photodegradation yields of organisms (*Salmonella, Pseudomonas*, yeast, fungi, total coliforms, fecal coliforms, heterotrophic bacteria) and ibuprophene, oxytetracycline removal yields were studied. The particle shapes and properties were investigated with field emission scanning electron microscope (FESEM) and fourier transform infrared spectrophotometer (FTIR), X-ray diffraction (XRD). The XRD pattern of Ag-Fe_3O_4 nanocomposites showed the same diffraction peaks at 26.9°, 33.0°, 38.3°, 55.1°, 65.7°, and 68.7° for Ag and at 28.26°, 34.53°, 44.01°, and 61.88° for Fe_3O_4, indicating a good coupling of Ag and Fe_3O_4 with no change in their crystal structure. The maximum organism and pollutant yields were detected at 1 mg/l Ag-Fe_3O_4 nanocomposite concentration, after 45 mins at a pH 7.00 and 5.00 for Ibuprophenin drug and Oxytetracycline antibiotic, respectively. 99% treatment yields were recorded for ibuprophene, oxytetracycline, and organisms during photocatalysis. The recovery studies with Ag-Fe_3O_4 NPs showed that all organisms and both pollutants can be used 120 times with the same yields. The photodegradation kinetics was found to be pseudo-first-order and the rate constants (k) for oxytetracycline and ibuprophene were calculated as 5×10^{-2} min^{-1}, and 5.02×10^{-2} min^{-1}, respectively. From 1.5 mg/l Ag- Fe_3O_4 nanocomposite 0,95 mg/l Fe^{3+} and 0,39 mg/l Ag +1 was leached during ibuprophene photodegradation. For oxytetracycline from 1.5 mg/l Ag- Fe_3O_4 nanocomposite 0,89 mg/l Fe^{3+} and 0,34 mg/l Ag +1 was leached.

Citation: Sponza DT, Öztekin R (2024) Photoremoval of Ibuprophenin and Oxytetracycline and some microorganisms from a pharmaceutical wastewater via Ag-Fe_3O_4 nanocomposites. Forefronts Proteom Sci. 1(1): 011-023. DOI: https://dx.doi.org/10.17352/fps.000002

Introduction

Pharmaceuticals are products used in large doses in daily life considered contaminants of emerging concern. Due to the large amounts of drugs consumed, the hydrogenic sources suffer from contamination processes that give rise to toxicological effects in humans despite their low concentrations [1]. Many medicines considered emerging contaminants are constantly detected in groundwater, wastewater treatment plants, and water supply. The inefficiency of conventional methods used in water treatment plants to remove the contaminant motivates the development of effective methods to treat effluent contamination [2]. According to the physico-chemical properties of drugs, their degradation products, and the characteristics of the soils, these substances can reach the groundwater and contaminate the aquifers or remain retained in the soil, thus affecting the ecosystem and humans through the food chain [3]. Additionally, the portion of medicines not assimilated by the organism, as well as chemical substances administered to animals, usually become part of wastewater. Consequently, different ways of removing medicines in water have been studied [4]. The residues of the pharmaceutical compounds administered to humans and animals—excreted as metabolites or in their native form—certainly contribute to water pollution [5]. Furthermore, the disposal of unused medications from households and manufacturing facilities also contributes to the spreading of PhACs in the environment. These residues fall within the group of the so-called emerging pollutants [6], together with illegal drugs, endocrine disruptors, personal care products, and household substances. Since PhACs are not easily degraded by the typical biological treatments in municipal wastewater treatment plants [7], together with all the toxic substances discharged from a treatment plant or a septic system, they can end up in surface waters or groundwaters that may ultimately be used as a source of drinking water [8].

Non-steroidal anti-inflammatory drugs are among the most frequently detected pharmaceuticals in environmental samples and the most widespread drugs in the world [9]. Ibuprofen (2-(4-(2-methylpropyl)phenyl)propanoic acid, hereinafter IBP) belongs to this family of medicines, and its concentration in the environment is reported to be between 10 and 160 ng L^{-1} [10]. Particularly, IBP is the sixth most abundant pharmaceutical detected in the inlet of wastewater treatment plants (WWTPs) in Italy, and in general, in the effluents of WWTPs, the IBP concentration ranges from 0.4 µg L^{-1} [11].

Ibuprofen is a nonsteroidal anti-inflammatory drug (NSAID) that is used to relieve pain, fever, and inflammation. This includes painful menstrual periods, migraines, and rheumatoid arthritis. It may also be used to close a patent ductus arteriosus in a premature baby [12]. It can be used orally (by mouth) or intravenously. It typically begins working within an hour. Ibuprofen is used primarily to treat fever (including postvaccination fever), mild to moderate pain (including pain relief after surgery), painful menstruation, osteoarthritis, dental pain, headaches, and pain from kidney stones. About 60% of people respond to any NSAID; those who do not respond well to a particular one may respond to another. Oxytetracycline works by interfering with the ability of bacteria to produce essential proteins. Without these proteins, the bacteria cannot grow, multiply, and increase in numbers. Oxytetracycline therefore stops the spread of the infection, and the remaining bacteria are killed by the immune system or eventually die.

Oxytetracycline is active against a wide variety of bacteria. However, some strains of bacteria have developed resistance to this antibiotic, which has reduced its effectiveness in treating some types of infections. Oxytetracycline (OTC) is a tetracycline antibiotic administered to dairy cows and bullocks for treatment and collective prophylaxis of bovine mastitis. 3-Indole Acetic Acid (IAA) is a plant hormone that regulates plant growth and has been used externally to improve agricultural yields [13].

The main sources of ibuprofen and oxytetracycline in the environment are derived from human excretions via urine or feces. Theoretically, if they could be completely removed in municipal Wastewater Treatment Plants (WWTPs), their potential ecological risks to the natural environment could be well controlled. Considering their wide use and ecological risks, the removal performance of municipal WWTPs on ibuprofen and acetaminophen should be well examined [14].

There are many ways to treat OTC in wastewater, such as absorption, oxidation, electrical degradation, and photocatalytic degradation [15]. For example, biochar has received extensive attention as an adsorbent, which could adsorb antibiotics and other pollutants in wastewater through high specific surface area and surface functional groups [16]. However, such physicochemical methods have disadvantages of high operational costs, limited removal effectiveness, or production of byproducts that may cause secondary pollution to the environment. In addition, conventional wastewater treatment plants are one of the largest energy consumers, using approximately 23% of public energy. Therefore, exploring more efficient, less harmful, and higher resource recovery methods is necessary to remove OTC in wastewater.

Biological wastewater treatment may provide an alternative solution to remove antibiotics. The techniques based on Advanced Oxidation Processes (AOPs) result in the oxidization of organic pollutants by generating extremely reactive species, the OH radicals. Over the past two decades, AOP-based treatments have been studied from both the experimental and the theoretical point of view [17]. Despite their great potential in the field of WWT and the recent advances in scientific knowledge, AOPs are still scarcely employed on pilot and industrial scales, particularly because of their cost (considering the equipment and the process). They can be energy- and material-intensive, and their residual streams often need further treatment and management [18]. Certain studies have focused on the photocatalytic degradation of oxytetracycline (OTC), also known as the classic antibiotic. For example, Ag-Fe_2O_3 nanocomposite photocatalysts were produced using a simple method at room temperature, which removed 96.57 % of OTC under visible light in 20 min [19].

Citation: Sponza DT, Öztekin R (2024) Photoremoval of Ibuprophenin and Oxytetracycline and some microorganisms from a pharmaceutical wastewater via Ag-Fe_3O_4 nanocomposites. Forefronts Proteom Sci. 1(1): 011-023. DOI: https://dx.doi.org/10.17352/fps.000002

In recent decades, much attention has been paid to the application of nanoparticles for environmental purposes. This is because nanosized materials have a large surface area-to-mass ratio and high reactivity. Thanks to these features, Nanoparticles (NPs) have been widely used as catalysts. Due to their non-specific action, NPs as adsorbents are capable of removing a wide variety of contaminants including organics, inorganics, and colloids such as bacterial cells. When a decrease in microbial contamination is a major goal, one can use some NPs with inherent disinfection capabilities such as magnetic nanoparticles. Therefore, the need for adding other disinfectants such as chlorine and ozone, which are associated with adverse side effects, may be eliminated.

Magnetite (Fe_3O_4) is the strongest magnetic species among the transient metal oxides. The reactive surface of iron-oxides allows for the adsorption of various impurities from the water environment. When used as NPs, called Fe_3O_4 NPs, they release Reactive Oxygen Species (ROS) such as superoxide radicals (O_2^-), hydroxyl radicals ($^{\cdot}OH$), hydrogen peroxide (H_2O_2), and singlet oxygen (O_2) that can decompose proteins and DNA in bacterial cells. Therefore, Fe_3O_4 NPs can exert their antibacterial effects through both physical adsorption and chemical disinfection. The magnetic feature of Fe_3O_4 NPs gives them an excellent separation property in the vicinity of an external magnetic field, which is essential for the removal of small-sized NPs from the effluent.

The composite of Ag NPs and Fe_3O_4 nanoparticles could be a promising material with good potential in biological and pharmaceutical sciences. Therefore, we are interested in describing the synthesis, characterizations, and applications of novel Ag NPs decorated magnetite nanocomposite (Ag/Fe_3O_4). The biomolecules of extract afford additional stability to the MNPs from unwanted oxidation and corrosion. The modified surface can easily have capped the Ag ions and in *situ* reduced and stabilized them without aggregations.

Combination of magnetic properties of magnetite NPs and antimicrobial features of nanosilver which predestinates these nanocomposites to be possibly used in disinfection and biomedical applications where they can be used for targeted transport of antimicrobial drug and/or for its removal by an external magnetic field [20]. They demonstrated that the Ag-Fe_3O_4 nanocomposite is a more effective antimicrobial agent since, regardless of its lower content of silver it effectively destroys pathogenic microorganisms due to the smaller size of its silver NPs compared.

Ag is a noble metal that exhibits a relatively weak oxidation behavior. In large sizes, it is a low-reactive metal. However, in nanoscales, its microbicidal characteristic is extremely enhanced due to the increased specific surface area [21]. Like Fe_3O_4 NPs, Ag NPs can exhibit their antibacterial activity through ROS generation [22]. In addition, other mechanisms have been mentioned such as the interaction of Ag-NPs with surface structures of bacterial cells and the reaction of released Ag ions with sulfur and phosphorous of cell macromolecules. Accordingly, Ag has been used successfully in previous studies as a bactericidal agent against Gram-negative bacteria, e.g., coliforms [23]. The easy separation of the magnetite product can facilitate the recovery of invaluable Ag particles. It has been stated that Ag in combination with Fe_3O_4 NPs can penetrate biofilms more easily than Ag alone [24]. Therefore, Fe_3O_4-Ag NPs can show enhanced characteristics for water and wastewater treatment purposes.

Shan et al., and Abboud, et al. investigated the effects of Ag_2O/Fe_3O_4 Magnetic nanocomposites to remove the organic compounds from wastewaters [25,26]. Padmavathy, et al. considered the combination of magnetic properties of magnetite NPs and antimicrobial features of nanosilver which predestinates these nanocomposites to be possibly used in disinfection and biomedical applications where they can be used for targeted transport of antimicrobial drugs and/or for its removal by an external magnetic field [27]. They demonstrated that the Ag-Fe_3O_4 nanocomposite is a more effective antimicrobial agent since, regardless of its lower content of silver, and effectively destroys the pathogenic due to a smaller size of its silver NPs compared to that found at the Ag and Fe_3O_4 nanocomposite solely. Padmavathy, et al. also found that Ag/Fe_3O_4 Magnetic nanocomposites exhibited bactericidal effects on microorganisms [27]. Simultaneous preparation of Ag/Fe_3O_4 core-shell nanocomposites with enhanced magnetic moment and strong antibacterial and catalytic properties remove effectively the organic compounds as reported by Hang and Anh [28]. Ag nanoparticles are extensively employed to degrade water pollutants due to their simple preparation, stable properties, and environmental friendliness. However, the narrow bandgap and low photogenerated carrier-separation efficiency of Ag limit its application in water treatment. Furthermore, using Ag as a powder photocatalyst makes it challenging to recycle [29,30]. Therefore, it is practically significant to develop a magnetic material to couple with Fe_3O_4 through heterojunctions to enhance the photogenerated carrier separation efficiency and fabricate an efficient and magnetically recoverable Ag-based photocatalyst. The small shell thickness and high shell porosity of the smallest Ag-Fe_3O_4 nanocomposite significantly improve mass diffusion making it an ideal substrate for highly sensitive detection of organic pollutants. had good stability and recyclability.

Therefore, this study is based on the assumptions given above, it was aimed to examine the effectiveness of Ag-Fe_3O_4 nanocomposite on the removals of ibuprophene and oxytetracycline present in raw pharmaceutical wastewater and some organisms like total coliforms, fecal coliforms, heterotrophic bacteria, *Pseudomonas*, yeast and fungi. The effects of some operational conditions (pollutant concentration, nanocomposite concentration, time, sunlight power, pH) on the yields of ibuprophene and oxytetracycline were studied. Furthermore, the structure and properties of the Ag-Fe_3O_4 nanocomposite were investigated with FESEM, TEM, XRD, and VSM analyses.

Materials and methods

Preparation of Ag-Fe_3O_4 nanocomposite

30 ml of H_2O was heated at 80°C and continuously stirred under N_2(g) atmosphere. Then, 0.67 g $FeCl_3.6H_2O$ and 0.32 g

Citation: Sponza DT, Öztekin R (2024) Photoremoval of Ibuprophenin and Oxytetracycline and some microorganisms from a pharmaceutical wastewater via Ag-Fe_3O_4 nanocomposites. Forefronts Proteom Sci. 1(1): 011-023. DOI: https://dx.doi.org/10.17352/fps.000002

$FeCl_2.4H_2O$ were added. When the solids were dissolved, 3 ml of concentrated ammonia solution was incorporated and the solution was stirred for 20 min. The particles were separated using a permanent magnet and the supernatant was discarded. The solid was washed three times with H_2O until the washing liquids were neutral. 0.32 g Fe_3O_4 NPs were suspended in 30 ml of H_2O. After 6,2 ml of diluted 0.022 g/l $AgNO_3$ solution was added, the mixture was stirred for 5 min and using the magnet was separated and washed several times with H_2O. Finally, Ag-Fe_3O_4 NPs were suspended in 30 ml of H_2O again.

Characterization of Ag-Fe_3O_4 nanocomposite

Field Emission Scanning Electron Microscope (FESEM) and Energy Dispersive X-Ray Analysis (EDX) analysis: The morphological features and structure of the synthesized catalyst were investigated by FESEM (FESEM, Hitachi S-4700), equipped with an EDX spectrometry device (TESCAN Co., Model III MIRA) to investigate the composition of the elements present in the synthesized catalyst. FESEM images were used to investigate the composition of the elements present in the synthesized Ag-Fe_3O_4 nanocomposite.

Transmission Electron Microscopy (TEM) analysis: The size and structure of the Ag-Fe_3O_4 nanocomposite samples were identified with TEM analysis. The obtained Ag-FeO_4 nanocomposite was collected and harvested by centrifugation (8000 rpm, 5 min), washed twice with deionized water, resuspended in ethanol (C_2H_6O), and dripped onto a carbon-coated copper (Cu) TEM grid. Vacuum drying then occurred to the Ag-Fe_3O_4 nanocomposite for 24 h at 25 °C room temperature. The dry samples on the Cu grid were viewed and examined by TEM analysis recorded in a JEOL JEM 2100 F, Japan under 200 kV accelerating voltage.

X-Ray Diffraction (XRD) analysis: Powder XRD patterns were recorded on a Shimadzu XRD-7000, Japan diffractometer using Cu Kα radiation (λ = 1.5418 Å, 40 kV, 40 mA) at a scanning speed of 1° /min in the 10 - 80° 2θ range. Raman spectrum was collected with a Horiba Jobin Yvon-Labram HR UV-Visible NIR (200 nm - 1600 nm) Raman microscope spectrometer, using a laser with a wavelength of 512 nm. The spectrum was collected from 10 scans at a resolution of 2 /cm. The zeta potential was measured with a SurPASS Electrokinetic Analyzer (Austria) with a clamping cell at 300 mbar.

Value Stream Mapping (VSM) analysis: In order to explain the magnetic property of Ag-Fe_3O_4 nanocomposite, the magnetic hysteresis curve was measured at 25 °C. The hysteresis loop exhibits ferromagnetic behavior with saturation magnetization (Ms) of 2.59 emu/g.

Fourier Transform Infrared Spectroscopy (FTIR) analysis: The FTIR spectra of samples were recorded using the FT-NIR spectroscope (RAYLEIGH, WQF-510). Experimental Ag-Fe_3O_4 nanocomposite samples were scanned using infrared light and their chemical properties were obtained in FTIR spectra.

Raman spectroscopy analysis: Raman spectra were excited by 514.5 nm radiation from an argon ion laser (Coherent, Innova) and collected in a backscattering geometry with a spectral resolution of 6 cm-1. Two holographic super-notch filters (Kaiser) were used to reject the Raleigh line. No polarizers were used. The laser beam was focused on the sample by a spot size of ca 5 µm - 10 µm. The reported Raman wavenumbers have uncertainties of 1.5 cm-1. The laser power reaching the sample surface was varied in the range of 7 - 60 mW. The typical acquisition time was 60s determination refers to the main peaks of the pattern diffractogram.

High Performance (or Pressure) Liquid Chromatography (HPLC) analysis: The concentrations of ibuprophene and oxytetracycline were performed using an HPLC (Agilent-1100). The samples were analyzed by HPLC with photodiode array and Mass Spectrometric Detection (MSD) using an Agilent 1100 HPLC system consisting of an automatic injector, a gradient pump, a Hewlett–Packard series 1100 photodiode array detector. The chromatographic conditions for the determination of ibuprophene and oxytetracycline concentrations were as follows: C-18 reverse phase HPLC column (Ace 5C18; 25-cm x 4.6-mm, 5 µm, mobile phase: 50/50 (v/v) methanol/organic-free reagent water). The experimental results were detected with an Agilent series 1100 VL online atmospheric pressure ionization electrospray ionization mass spectrometer.

Determination of Ag-Fe_3O_4 nanocomposite size:

Determination with Scherrer's equation:

X-ray diffraction can be used to determine the size of a crystal (crystallite size) with a phase

certain. Equation 1 gives the Scherrer's equation.

$$D = \frac{K.\lambda}{\beta.\mathrm{Cos}\theta} \quad (1)$$

Where,

D is the crystallite size (nm), K is the Scherrer constant (0.9), λ is the wavelength of the X-ray used (0,15406 nm, β is the full width at half maximum (FWHM) radians and θ is the peak position radians.

Determination with Williamson Hall plot: Williamson and Hall proposed a method for obtaining size and strain broadening by considering peak width as a function of 2θ. By plotting FW(s)×cosθ on the y-axis against sinθ on the x-axis, we get the strain component from the slope and the particle size component from the y-intercept (Equation 2).

$$\Delta\theta.\cos\theta = \frac{k.\lambda}{D_{VHP}} + 4P\sin\theta \quad (2)$$

Where, Δθ is full width at half maximum (FWHM) of Bragg peaks, in radians and eliminating the broadening from instrumental contribution, θ is the angle of peak position, λ(= 1.5406 Å) is the wavelength of the X-ray, D_{WHP} is average crystallite size, k is constant value 0.9 by presuming spherical nature of powders and η is lattice strain.

Citation: Sponza DT, Öztekin R (2024) Photoremoval of Ibuprophenin and Oxytetracycline and some microorganisms from a pharmaceutical wastewater via Ag-Fe_3O_4 nanocomposites. Forefronts Proteom Sci. 1(1): 011-023. DOI: https://dx.doi.org/10.17352/fps.000002

Photocatalytic degradation of Ibuprophene, Oxytetracycline, and some organisms

The photodegradation of **Ibuprophene and Oxytetracycline** was investigated by employing a synthesized sample as a photocatalyst. To prepare samples containing the aforementioned pollutants and microorganisms the raw water was diluted with distilled water. Before introducing the Ag-Fe_3O_4, the photo absorbance was measured to assess the gradual reduction in the photoabsorption curve resulting from the photocatalytic degradation of pollutants. Subsequently, an increasing amount of the nanocomposite was mixed with pharmaceutical industry raw wastewater increasing time intervals under standard temperature and pH conditions. The nanocomposite was separated using centrifugation, and absorbance values were recorded.

Measurement of leach ions (Fe +3 and Ag +1) concentrations

Triple Quadrupole ICP-MS coupled to an NWR193 excimer laser ablation system (Elemental Scientific Lasers, Bozeman, USA) was used for Fe^{+3} and Ag +1 concentrations. The ICP-MS was purged with Heat 2 l min^{-1} for 5 min, then reconnected and the system flushed at normal gas flow rates for at least two hours before continuous analysis. 8900 Triple Quadrupole ICP-MS with two chambers was used. The power was 1550 W, sampling depth and gas flow rates were 5 mm and l /min.

Photodegradation kinetic of ibuprophene and oxytetracycline

Equation 3 demonstrates the first pseudo-order kinetic of the photodegradation of **ibuprophene and oxytetracycline using Ag-Fe_3O_4 nanocomposite**

under direct sunlight irradiation.

$$\ln(Co/Ct) = kt \quad (3)$$

t is the time (min), C_o is the pollutant concentration at the beginning before photooxidation (mg/l), C_t is the organic pollutant concentration after t time photooxidation, and k is the pseudo-first-order rate constant.

Microorganism enumeration

The organism identification and enumeration were performed by following Standard Methods (2022) [31].

Results and discussions

Physicochemical Properties of Ag-Fe_3O_4 NPs

FESEM analysis: Field emission scanning electron microscopy analysis was performed to check the presence of Ag in the Ag-Fe_3O_4 nanocomposite. The FESEM image shows that Fe3O4 nanometal oxide and Ag nanoparticles are capsulated by flexible sheets with crinkled structures. The size and morphology of Ag-Fe_3O_4 core-shell nanocomposite particles contain multifaceted particles with a size of 30 nm - 40 nm. In comparison to the images of Fe (III) with Fe (II) in the Ag-Fe_3O_4 nanocomposite, it was observed smaller size (30 nm - 40 nm), due to the smaller ionic radius of Fe(III) than Fe(II) (40 nm - 50 nm). Figure 1a shows the image for Fe_3O_4, while Figure 1b shows the formation of Ag-Fe_3O_4 NPs where the Ag appears as spherical, and shiny due to its elevated atomic number.

TEM analysis results: TEM images were performed to determine the morphologies of Fe_3O_4 NPs and Ag-Fe_3O_4 NPs. These particles contain a uniform structure with certain void regions between the iron oxide core and the Ag shell. The thickness of silver was measured as 7 nm, and the diameter of the Fe_2O_3 nanoparticle was found to be 25 nm - 35 nm. According to these observations, the size of Ag- Fe_3O_4 nanoparticles was around 32 nm 42 nm. TEM images are presented in **Figure 2**. As can be observed, Fe_3O_4 NPs and Ag-Fe_3O_4 nanocomposite shapes were almost semi-spherical. The TEM image of Ag-Fe_3O_4 NPs appeared darker than that of Fe_3O_4 NPs [29].

EDX analysis: Energy dispersive X-ray spectroscopy (EDX) graphs for Ag-Fe_3O_4 NPs are presented in Figure 3. A BET analysis was performed to determine the surface area of the Ag-Fe_3O_4 nanocomposite. This value was calculated as 117.598 m^2/g. EDX examination confirmed that various components were effectively deposited on the surface of the Ag-Fe_2O_3 nanocomposite [26-29]. The EDX spectra revealed

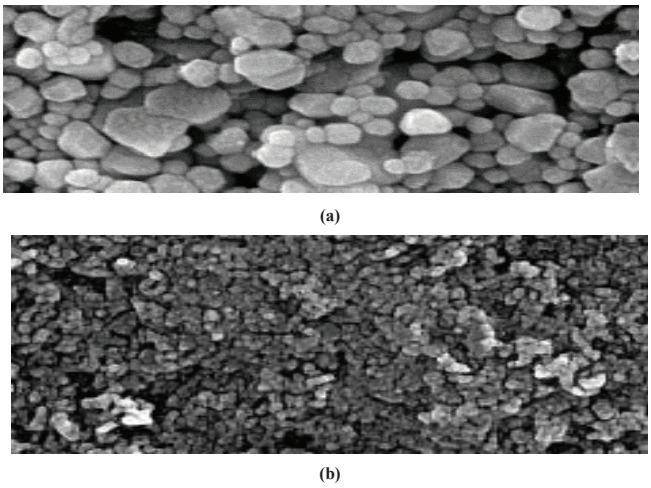

(a)

(b)

Figure 1: FESEM images of (a) Fe_3O_4 NPs and (b) Ag-Fe_3O_4 NPs.

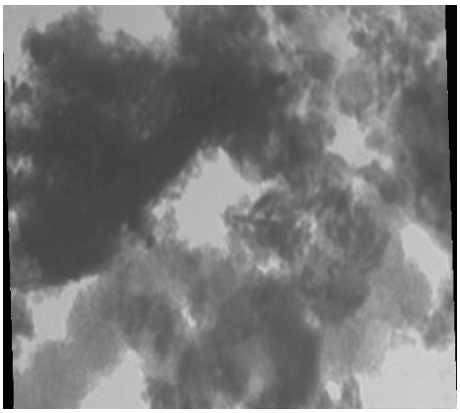

Figure 2: TEM analysis results of Fe_3O_4 and Ag-Fe_3O_4 NPs.

Citation: Sponza DT, Öztekin R (2024) Photoremoval of Ibuprophenin and Oxytetracycline and some microorganisms from a pharmaceutical wastewater via Ag-Fe_3O_4 nanocomposites. Forefronts Proteom Sci. 1(1): 011-023. DOI: https://dx.doi.org/10.17352/fps.000002

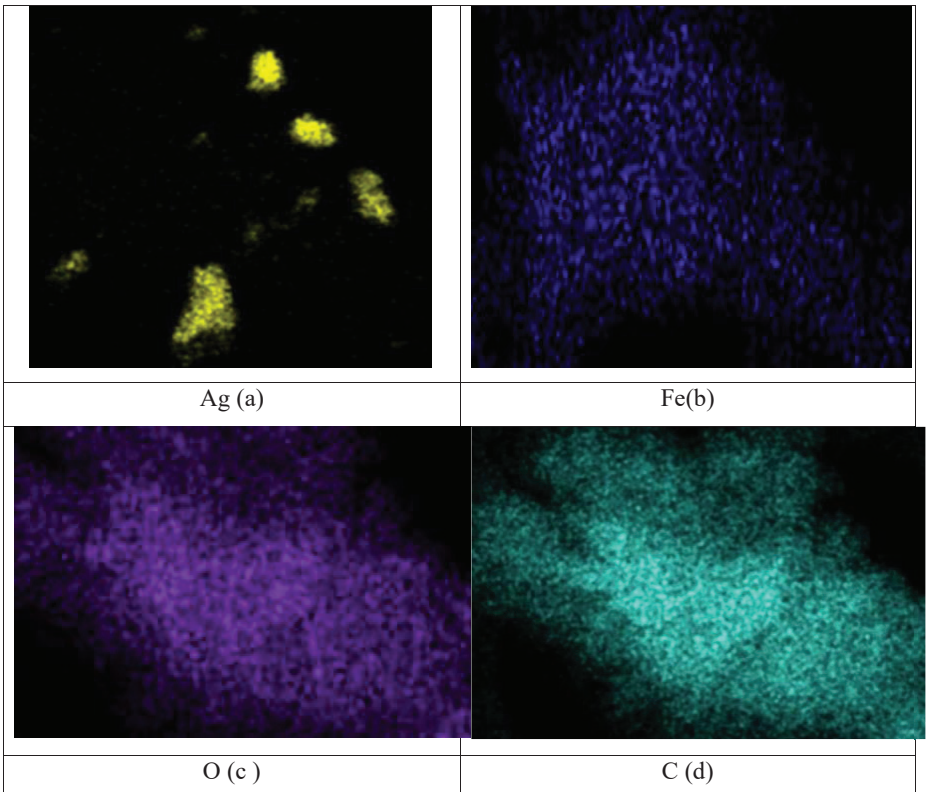

Figure 3: EDX spectra of Ag-Fe_3O_4 NP and nanocomposite elements (Ag -a, Fe-b, O-c and C-d).

the existence of several well-defined peaks in the Ag-Fe_2O_3 nanocomposite that were connected to silver, iron, oxygen, and carbon components (Figure 3).

XRD analysis results: Figure 4 presents the X-ray diffraction spectra of Fe_3O_4 nanometal oxide and Ag-Fe_3O_4 nanocomposite. The diffraction pattern of the Fe_3O_4 exhibited maximum abundances in the 2θ positions of 24.31, 34.07, 36.09, 41.77, 50.09, 55.07, 58.45, and 64.02°, which are related to the (022), (106), (115), (116), (026), (118), (019), and (216) planes. These points were identified as hematite (Fe_3O_4) nanoparticles (JCPDS card no. 39–1346) [29]. In this step, the diameter of the Fe_3O_4 was calculated as 33,8 nm at illustrated peaks at a diffraction peak of 2θ = 36.09° using the Scherrer equation. The diameter of Ag-Fe_3O_4 was also measured by the Williamson Hall plot as 33,9 nm. It can be noted that the values of the average crystallite size obtained from the Scherrer equation and Williamson Hall plot are in good agreement with the results of the TEM analysis. The values of crystallites obtained from the two models are in good agreement with the values obtained from FE-SEM. We suggest that these two models are the best models for the evaluation of the crystallite size of the Ag-Fe_3O_4 nanocomposite.

The diffraction pattern of Ag-Fe_3O_4 nanocomposite peaks throughout at 2θ positions of 31.06, 36.69, 44.09, 55.82, 58.42, and 63.34° are related to (222), (3131), (403), (425), (514), and (444) planes. These results exhibited significant correlations to magnetite (Fe_3O_4) nanoparticles with an inverse spinel structure (JCPDS card no. 89 - 0691 [30,32]. The crystalline

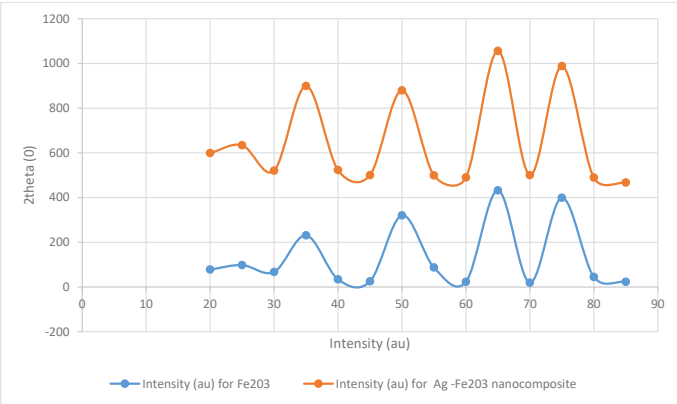

Figure 4: The XRD pattern of Fe_3O_4 s and Ag-Fe_3O_4 nanocomposite.

lattice of Fe_3O_4 was configured for the observed diffraction peak at 2θ = 37.34° and obtained to be 31 nm. The appearance of silver throughout the crystalline structure of synthesized Ag-Fe_3O_4 nanocomposite illustrated peaks at 2θ positions of 39.01, 43.94, 65.1, and 73.01°. The crystallite size of Ag-Fe_3O_4 nanocomposite is higher compared to that of Fe_3O_4 due to the ionic radius of Fe(III) (0.61 Å) being bigger than that of Fe(III) (0.55 Å). It was observed that the intensity of silver peaks was higher than that of Fe_3O_4 peaks, due to the Ag covering the whole surface of the Fe_3O_4 (Figure 4).

In order to detect the stability of the synthesized photocatalyst, the XRD peaks before the photocatalysis and after 20 times of sunlight irradiation during the photodegradation

Citation: Sponza DT, Öztekin R (2024) Photoremoval of Ibuprophenin and Oxytetracycline and some microorganisms from a pharmaceutical wastewater via Ag-Fe_3O_4 nanocomposites. Forefronts Proteom Sci. 1(1): 011-023. DOI: https://dx.doi.org/10.17352/fps.000002

of ibuprophene and oxytetracycline in pharmaceutical wastewater were performed (Figure 5). The same peaks were obtained again. The stability of the Ag-Fe_3O_4 nanocomposite is confirmed. Therefore, the produced nanocomposite has the potential to photodegrade the raw industrial wastewater.

VSM analysis results: The Vibrating Sample Magnetometer (VSM) analysis was conducted to determine the magnetic properties of NPs (Figure 6). The magnetic properties of Fe_3O_4 and Ag-Fe_3O_4 nanocomposite were evaluated through the application of vibrating sample magnetometry. Fe_2O_3 exhibited a magnetic saturation (Ms) value of 1.87 emu/g while the saturation magnetization of Ag-Fe_2O_3 was recorded as 0,87 emu/g (Figure 6). The existence of silver in the Ag-Fe_3O_4 nanocomposite lowered the saturation magnetization of samples, due to spin disturbance in the upper surfaces of the Fe_2O_3. Therefore, the observed reduction in Ms value in the Ag-Fe_3O_4 nanocomposite was caused by shielding effects, due to the observance of the silver in the surrounding of the Fe_3O_4. The hysteresis loop analysis of VSM exhibited the magnetic structure of the Ag-Fe_3O_4 nanocomposite.

FTIR analysis: Figure 7 shows the FTIR spectrum for Fe_3O_4 and Ag-Fe_3O_4 nanocomposite. The functional groups and potential chemical variations of active components showed that Ag-Fe_2O exhibited spectral disturbances between 400 and 4000 cm^{-1}. The intense broad band was observed from 3400 to 2990 cm^{-1} and the spectrum was relevant with H-bonded and O–H vibrations of Ag and O groups. The presence of a slight shift at 2095 cm^{-1} indicated –C=C– stretch variability. The FTIR analysis further confirmed the presence of functional groups (CO– stretch) containing carboxylic acid, and ester, with maximum peak values at 1092–1007 cm^{-1}. The presence of carboxylic acid bestowed hydrophilic functionality, leading to enhanced stability of the Fe_2O_3 NPs. The study also identified characteristic stretching vibrations for Ag–O bonds during 610 to 420 cm^{-1}. The spectra exhibit two distinctive bands at 436 cm^{-1} and 544 cm^{-1}, corresponding to the Fe–O stretching vibration mode in iron oxide, which is attributed to both Fe_2O_3 NPs and Ag-Fe_2O_3 nanocomposite at 529 cm^{-1} and 456 cm^{-1} bands, respectively.

Raman spectroscopy results: The Raman analyses showed that only a strong peak at 665 cm-1 can be attributed to the

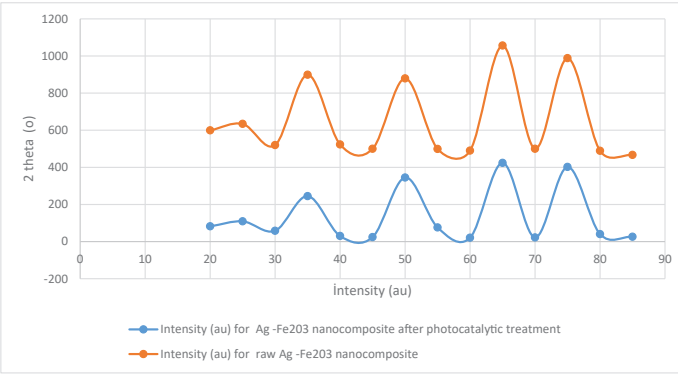

Figure 5: XRD peaks of raw Ag - Fe_3O_4 nanocomposite before photodegradation and after 20 times photooxidation under sun ligth for pharmaceutical wastewater containing ibuprophene drug and oxytetracycline antibiotic.

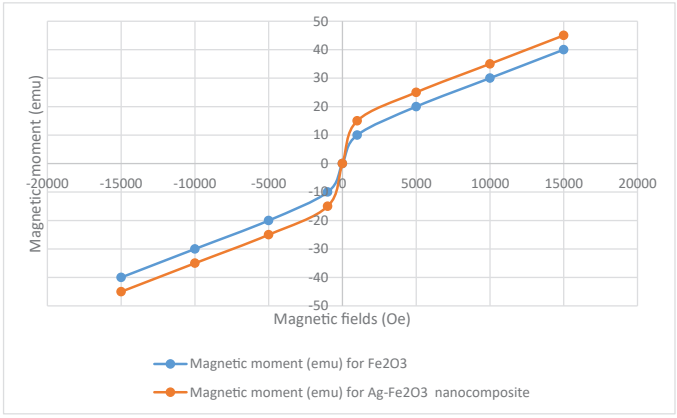

Figure 6: Magnetic hysteresis loops of Fe_3O_4 and Ag-Fe_3O_4 nanocomposite.

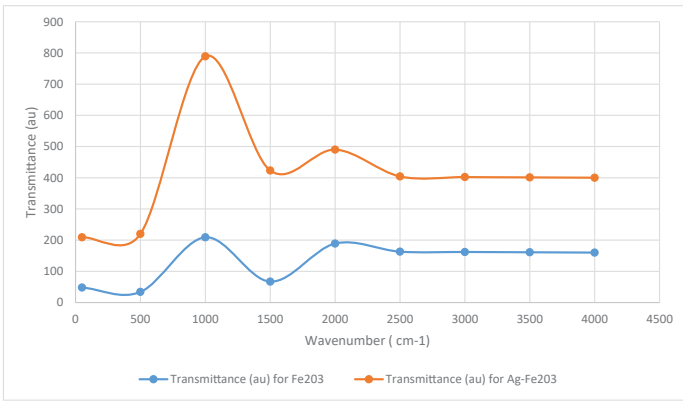

Figure 7: FTIR spectra of Fe_3O_4 (blue) and Ag-Fe_3O_4 nanocomposite (red).

spinel crystalline structure of Ag-Fe_3O_4 nanocomposite (Figure 8). The Raman spectrum of Ag-Fe_3O_4 nanocomposite after exposure 30 times to photocatalysis showed several peaks at 187, 360, 490, 680, and 1380 cm-1. These peaks can be attributed to Ag-Fe_3O_4 nanocomposite. The peaks around 680 and 1380 are characteristic bands of Ag-Fe_3O_4.

Anion leaching: The ICP- MS analysis showed that from 1.5 mg/l Ag-Fe_3O_4 nanocomposite 0,95 mg/l Fe^{3+} and 0,39 mg/l Ag +1 was leached (data not shown) in the photocatalytic removal of ibuprophene. For oxytetracycline from 1.5 mg/l Ag-Fe_3O_4 nanocomposite 0,89 mg/l Fe^{3+} and 0,34 mg/l Ag +1 were leached (data not shown). Compared with homogeneous catalysts, an important advantage of heterogeneous catalysts is that they can be easily separated from the treated water, making the process economically viable. It was mentioned that it was examined for metal leaching from several solid catalysts and further investigated the influence of the leached metal ions on the mineralization of organic compounds during continuous photocatalysis. The water matrix has been demonstrated to play an important role in metal leaching. The homogeneous catalytic effect resulting from the leached metal ions was found to be significant. It can be said that the stability of our nanocomposite and the effects of the leached ions must be carefully examined during the photocatalytic degradation of organic contaminants like drugs and antibiotics.

Citation: Sponza DT, Öztekin R (2024) Photoremoval of Ibuprophenin and Oxytetracycline and some microorganisms from a pharmaceutical wastewater via Ag-Fe_3O_4 nanocomposites. Forefronts Proteom Sci. 1(1): 011-023. DOI: https://dx.doi.org/10.17352/fps.000002

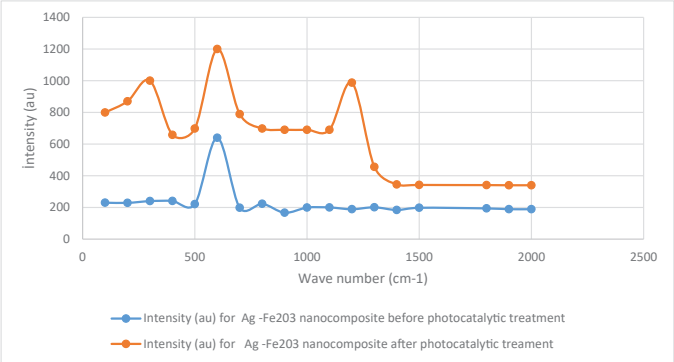

Figure 8: Raman Spectra of Ag-Fe_3O_4 nanocomposite before and after photocatalytic treatment.

Photocatalytic reaction mechanism: Under sunlight irradiation, Ag and Fe_3O_4 on the surface of Ag/Fe_3O_4 are excited from the Valence Band (VB) to the Conduction Band (CB), generating photogenerated electrons (e^-) and leaving behind holes (h^+) [32]. As the E_{CB} of Ag is -0.67 eV, which is more negative than that of Fe_3O_4, i.e., 0.54 eV, and the E_{VB} of Ag is 2.03 eV, which is more negative than that of Fe_3O_4, i.e., 2.14 eV, photocatalysis formed due to the band offset when the two are coupled. The h^+ on the Fe_3O_4 valence band transfers to the Ag valence band, and the e^- on the Ag conduction band transfers to the Fe_3O_4 conduction band. This accelerates the separation efficiency of the photogenerated electrons and holes. These electrons and holes attend to other redox reactions. The e^- on the Fe_3O_4 conduction band reacts with the dissolved oxygen and water in the liquid to form H_2O_2 and OH^-. H_2O_2 can then further participate in the photocatalytic reaction, while the h^+ on the Ag valence band reacts with H_2O to generate ·OH free radicals and H^+. H_2O_2 is generated in the photocatalytic reaction, dissolved in water O_2 to generate Fe^{3+}, $\cdot O_2^-$, and ·OH, respectively. Then H_2O_2 can reduce Fe^{3+} to replenish the consumed Fe^{2+} and O_2 and generate H^+, as a result, the reaction can be cycled. The large amounts of ·OH, and $\cdot O_2^-$ generated by the photocatalytic reactions can further participate in the oxidation and degradation of ibuprophene and oxytetracycline, decomposing them into smaller harmless compounds. The specific reaction process can be defined with Equations between 4 and 10:

$$Ag/Fe_3O_4 + hv \rightarrow e^- + h^+ \; Ag/Fe_3O_4 + hv \rightarrow e^- + h^+ \quad (4)$$

$$h^+ + H_2O \rightarrow \cdot OH + H + h^+ + H_2O \rightarrow \cdot OH + H^+ \quad (5)$$

$$2e^- + O_2 + 2H_2O \rightarrow H_2O_2 + 2OH - 2e^- + O_2 + 2H_2O \rightarrow H_2O_2 + 2OH^- \quad (6)$$

$$\cdot O_2 + OT/IBP \rightarrow \text{Degraded products} \cdot O_2 + OT/IBP \rightarrow \text{Degraded products} \quad (7)$$

$$H_2O_2 + 2Fe^{3+} \rightarrow 2Fe^{2+} + O_2 + 2H + H_2O_2 + 2Fe^{3+} \rightarrow 2Fe^{2+} + O_2 + 2H^+ \quad (8)$$

$$\cdot O_2 + OT/IBP \rightarrow \text{Degraded products} \cdot O_2 + OT/IBP \rightarrow \text{Degraded products} \quad (9)$$

$$\cdot OH + OT/IBP \rightarrow CO_2 + H_2O \quad (10)$$

Where OTC is oxytetracycline, IBP is ibuprophene.

Photodegradation kinetic of oxytetracycline and ibuprophene by Ag-Fe_3O_4 nanocomposite: The photodegradation kinetics of oxytetracycline and ibuprophene were determined under visible light. Figure 9 exhibited the kinetics of the photodegradation of oxytetracycline and ibuprophene in the presence of 1.5 mg/l Ag- Fe_3O_4 nanocomposite. The graphs of ln (C_t/C_o) were plotted as a function of the reaction time. The linearization of the results confirms the first pseudo-order kinetics of the photo-degradation of oxytetracycline and ibuprophene. A good correlation to the first pseudo-order reaction kinetics ($R^2 = 0.99$ for oxytetracycline, $R^2 = 0.99$ for ibuprophene was found. The calculated pseudo-first-order rate constants (k) of oxytetracycline and ibuprophene are 5×10^{-2} min^{-1}, and 5.02×10^{-2} min^{-1}, respectively.

Effects of operational conditions on the yields of pollutants and organisms

Effect of increasing ibuprophene and oxytetracycline concentrations on the photodegradation yields of ibuprophene and oxytetracycline: The pollutant concentrations were increased from 10 mg/l up to 600 mg/l to detect the optimal pollutant dose for maximum ibuprophene and oxytetracycline photodegradation yields (Table 1). The maximal ibuprophene

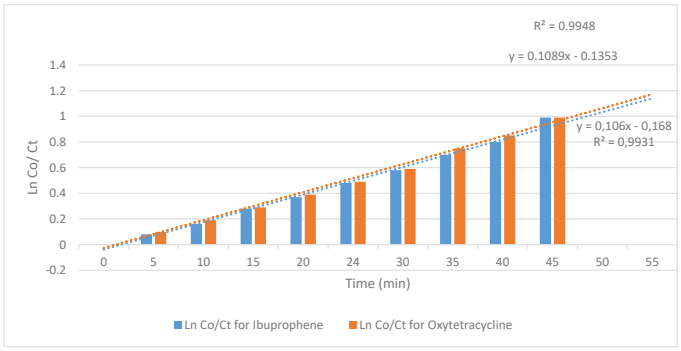

Figure 9: Phtodegradation kinetic of oxytetracycline and ibuprophene (first pseudo-order kinetic).

Table 1: Effect of ibuprophene and oxytetracycline concentrations on the photodegradations yields.

Ibuprophene oxytetracycline concentrations (mg/l)	Photodegradation efficiency of ibuprophene (%)	Photodegradation efficiency of oxytetracycline (%)
10	90	88
20	93	90
30	93	92
50	94	93
70	95	93
100	97	96
200	97	95
300	98	98
350	96	94
400	95	93
450	95	90
500	95	90
600	94	90

Citation: Sponza DT, Öztekin R (2024) Photoremoval of Ibuprophenin and Oxytetracycline and some microorganisms from a pharmaceutical wastewater via Ag-Fe_3O_4 nanocomposites. Forefronts Proteom Sci. 1(1): 011-023. DOI: https://dx.doi.org/10.17352/fps.000002

and oxytetracycline yields were detected at 300 mg/l. 98% maximum ibuprophene and oxytetracycline photodegradation yields were measured after 45 min contact time, at 1,5 mg/l Ag-Fe_3O_4 nanocomposite concentration. Higher pollutant concentrations lower the relative surface area accessible to environmental factors that lead to photofading. Therefore, an increase in the pollutant concentration leads to slower photodegradation yields. Increased pollutant concentrations may also lead to higher absorption on the surface and weaker interactions between the pollutant and nanocomposite, resulting in lower reaction rates. In heterogeneous photocatalytic systems, it was found that an increase in the pollutant concentration leads to reduced photodegradation efficiencies and lower reaction rates [33]. At high pollutant levels the rate-limiting step of the formation of hydroxyl radicals on the photocatalytic surface can be explained as follows: as the initial pollutant concentration increases fewer photons will reach the catalyst surface due to absorbance by the pollutant molecules, therefore, fewer reactive radicals are produced by the catalyst, leading to slower photodegradation rates [34].

Effect of increasing Ag-Fe_3O_4 nanocomposite concentrations on the photodegradation of ibuprophene and oxytetracycline: The Ag-Fe_3O_4 NP concentrations were increased from 0.05 mg/l up to 6.0 mg/l to detect the optimal nanocomposite for maximum ibuprophene and oxytetracycline photodegradation yields (Table 2). The ibuprophene and oxytetracycline concentrations were chosen as 300 mg/l at a constant concentration. 99% maximum ibuprophene and oxytetracycline photodegradation yield was measured after 45 min contact time, at 1 mg/l Ag-Fe_3O_4 nanocomposite concentration.

The photocatalyst loading is a very important phenomenon during photodegradation. An increase in the amount of catalyst leads to higher photodegradation efficiencies and increased reaction rates as more active sites are provided for the adsorption of pollutant molecules. The initial reaction rates were found to increase proportionally with the amount of the catalyst, however, beyond a certain critical point, both the rate and efficiency of the photodegradation reaction either level off or even begin to drop [34]. An increase in the suspension's turbidity, leads to more dominant light scattering phenomena, resulting in limited light absorption by the photocatalyst surface. An optimum amount of photocatalyst does exist and should be determined first, not only to ensure efficient photodegradation but also to avoid unnecessary use of catalyst excess.

Effect of Contact time on the photodegradation of ibuprophene and oxytetracycline: In order to detect the optimum photodegradation time for both organics the photocatalytic studies were performed between 1 and 90 min. For maximal ibuprophene and oxytetracycline yields the optimal photodegradation time was detected at 45 min.

From there, the percentage of adsorption remains constant until 90 min (Table 3). It was observed that ibuprophene and oxytetracycline concentrations significantly decreased as the time of the reaction continued. At high photodegradation times, the pollutant yields decreased. This may be due to the formation of several layers on the surface of the nanocomposite, meaning that the photodegradation layer became thicker on the surface of the catalyst, and also, this hinders the light from reaching the active sites on the surface of the photocatalyst easily and retard the excitation of the h–e pair [36,39].

Effect of pH on ibuprophene and oxytetracycline adsorption on Ag-Fe_3O_4 nanocomposite: The effect of pH on the photodegradation of ibuprophene and oxytetracycline with Ag-Fe_3O_4 nanocomposite was studied within the pH ranges varying between 2.0 and 9.0. The highest degree of adsorption was achieved at pH = 7.0 (Table 4). The dependence of photodegradation on pH is associated with the point of zero charges of the Ag-Fe_3O_4 nanocomposite and the pKa of the ibuprophene. The PZC is 6.93 for Ag. The ibuprophene is a weak acid (pKa = 5.2) and exists as a neutral species for pHpKa41. For pH > 8.0, ibuprophene is deprotonated and the Ag surface

Table 2: Effect of Ag-Fe_3O_4 nanocomposite concentration on the photodegradation of 300 mg/l ibuprophene and oxytetracycline photodegradations.

Ag-Fe_3O_4 nanocomposite concentration (mg/l)	Photodegradation efficiency of ibuprophene (%)	Photodegradation efficiency of ibuprophene (%)
0.05	90	88
0.1	92.7	90
1.0	99	99
1.5	98	96
2.0	98	96
2.5	97	95
3.0	97	95
3.5	96	95
4.0	96	94
4.5	95	93
5.0	95	90
5.5	95	90
6.0	94	90

Table 3: Effect of Contact time on the photodegradation of ibuprophene and oxytetracycline.

Photodegradation time (min)	Photodegradation efficiency of ibuprophene (%)	Photodegradation efficiency of ibuprophene (%)
5	80	78
10	85	80
15	87	83
20	90	88
25	95	92
35	99	94
45	99	99
55	99	99
65	98	95
75	97	93
85	95	92
90	95	90

Citation: Sponza DT, Öztekin R (2024) Photoremoval of Ibuprophenin and Oxytetracycline and some microorganisms from a pharmaceutical wastewater via Ag-Fe_3O_4 nanocomposites. Forefronts Proteom Sci. 1(1): 011-023. DOI: https://dx.doi.org/10.17352/fps.000002

Table 4: Effect of pH on the photodegradation yields of 300 mg/l ibuprophene and 300 mg/l oxytetracycline separately in the presence of 1 mg/l Ag-Fe_3O_4 nanocomposite.

pH	Ibuprophene	Oxytetracycline
	Photodegradation yields (%)	Photodegradation yields (%)
4.0	67.00	56.00
5.0	68.00	99.00
6.0	60.00	54.00
7.0	99.00	50.00
8.0	64.00	43.00
10.0	40.00	40.00

becomes negatively charged, thus leading to an electrostatic repulsion which reduces the photodegradation efficiency [33]. For pH values greater than pKa but lower than PZC, electrostatic attraction between anionic ibuprophene and the positively charged surface of Ag NPs improves the adsorption capacity. However, the influence of the initial pH of oxytetracycline photodegradation with Ag-Fe_3O_4 nanocomposite was different from the ibuprophene. When the pH was lower than 5.0, the adsorption rate increased with pH increasing. When pH was equal to 5.0, the adsorption rate reached the maximum. The maximum removal yields for ibuprophene and oxytetracycline were 99%.

Photodegradation in solution may be significantly influenced by the solution pH or other reducing agents. Redox-active groups can be protonated or deprotonated in acidic or alkaline pH, respectively, resulting in different forms, which may be less susceptible to photodegradation. In heterogeneous photocatalytic systems, photodegradation is indirectly influenced by the solution pollutants, depending on both the solid catalyst and the dissolved organics. In particular, pH affects the electrostatic interactions between the molecules on the surface of the photocatalyst and the pollutant molecules, thus, the photodegradation capacity of the catalyst is altered [32]. Therefore, at a lower pH protonation of the photocatalyst will take place, leading to a positively charged surface, whereas at higher pH values a negatively charged surface will be formed.

İntensity of light power: Light of higher intensities leads to higher photodegradation efficiencies and accelerated reaction rates, as more photons are introduced into the system An important definition that can be used to quantify and compare the light stability between compounds, is the quantum yield of photodegradation: the number of absorbed photons leading to a molecular reaction relative to the total number of photons absorbed. Low quantum yields, end with low photodegradation since absorption of a photon and the absorbed energy are more likely to be converted to heat or emitted a fluorescence. In this study, the maximal photodegradation yields were detected at a sunlight power of 60 W/m^2 (Table 5).

Reuse and recycling studies of Ag-Fe_3O_4 nanocomposites: The recoveries of the ibuprophene and oxytetracycline from the surface of the nanocomposite were performed at 1 ml HNO_3 solution, at pH = 1.0. When the ibuprophene and oxytetracycline recoveries are carried out, a magnet is used for separation from the aqueous and then decanted. Then, 1 ml HNO_3 solution is added and the mixture is sonicated for 3 min. After, the nanocomposite was removed with the magnet and the acid solution was quantified by HPLC. Recycling studies were carried out showing that Ag-Fe_3O_4 nanocomposites can be used during 120 additional successive photocatalytic cycles without losing photodegradation capacity. On the 140th photocatalytic cycle, the photodegradation yields decreased from 99% to 97% for both pollutants. The photodegradation rates declined slightly after 120th cycles (Table 6) This showed that Fe_3O_4-Ag nanocomposite was effective in the recycling studies.

Removal of microorganisms

The photo removals of organisms present in raw pharmaceutical wastewater (*Salmonella*, *Pseudomonas*, yeast, fungi, total coliforms, fecal coliforms, heterotrophic bacteria) were investigated under operational conditions where maximum photodegradation yields for ibuprophene and oxytetracycline were detected (300 mg/l pollutant concentration, 1 mg/l nanocomposite concentration, pH 7.00 and 5.00, 45 mn photooxidation time). 99% removal yields were detected for all types of organisms under optimized conditions (Table 7).

Ag has been utilized as a bacteriostatic material because Ag ions can kill bacteria by punching holes in bacterial membranes and damaging them inside. Apart from its excellent antibacterial effect, harmful byproducts are not generated during the antibacterial process of Ag sterilization as chloride derives. In general, the antimicrobial efficacy of Ag ions can be enhanced

Table 5: Effect of sun light power on the photodegradation yields of 300 mg/l ibuprophene and 300 mg/l oxytetracycline separately in the presence of 1 mg/l Ag-Fe_3O_4 nanocomposite.

Sun light power	Ibuprophene	Oxytetracycline
	Photodegradation yields (%)	Photodegradation yields (%)
10	67.00	56.00
20	69.00	78.00
30	80.00	79.00
60	99.00	99,00
80	64.00	43.00
100	40.00	40.00

Table 6: Reuse of Ag-Fe_3O_4 nanocomposites.

Cycles	Photodegradation efficiency of ibuprophene (%)	Photodegradation efficiency of ibuprophene (%)
1	99	99
3	99	99
5	99	99
10	99	99
15	99	99
20	99	99
40	99	99
60	99	99
90	99	99
120	99	99
140	97	96
160	96	95

Citation: Sponza DT, Öztekin R (2024) Photoremoval of Ibuprophenin and Oxytetracycline and some microorganisms from a pharmaceutical wastewater via Ag-Fe_3O_4 nanocomposites. Forefronts Proteom Sci. 1(1): 011-023. DOI: https://dx.doi.org/10.17352/fps.000002

Table 7: Removal of microorganisms.

Name of organisms	Numbers in raw pharmaceutical wastewater (colony/ ml)	Removal yields (%)
Salmonella,	340	99
Psuedomonas	180	99
Total yeast	50	99
Total fungi	34	99
Total coliforms	10.000	99
Fecal coliforms	8.000	99
Total heterotropic bacteria	20.000	99

by increasing the content of Ag particles. If Ag particles can be manipulated in some efficient way to increase their contact surface or frequencies with bacteria, a higher antibacterial effect could be expected with the lower concentration of Ag particles and the risks of environmental contamination from Ag particles can be reduced. Over the past decades, magnetic NPs have been widely applied to magnetic targeting medical tools, magnetic resonance imaging agents, and the carriers of the Ag-loading antimicrobials]. Among the various magnetic support materials, Fe_3O_4 nanostructure has gained much attention in the fields of environmental engineering due to its stable magnetic properties and favorable biocompatibility. Silver-coated Fe_3O_4 NPs as functional antimicrobial agents have now become an important research topic. The use of a magnetic field is extremely versatile because the field strength and its orientation can be controlled. The results showed that the antibacterial effect of Ag in these aqueous suspensions was greatly improved by magnetically stirring the Ag/Fe_3O_4 NPs in the magnetic manipulation system. Therefore, utilizing magnetically-controlled Ag/Fe_3O_4 NPs in aqueous suspensions can be applied to water purification and other sterilization-related objectives. Magnetic nanoparticles with a core/shell structure promise many applications due to their multi-functionality. Iron-oxide nanoparticles play a major role in many areas of chemistry, physics, and materials science. Fe_3O_4 (Magnetite) is one of the magnetic nanoparticles. Different reports are demonstrating that magnetic Fe_3O_4 can be used for wastewater purification, such as to adsorb arsenite, arsenate, cadmium, and nickel, used to remove alkalinity and hardness, desalination, decolourisation of pulp mill effluent and removal of natural organic compounds. After adsorption, Fe_3O_4 can be separated from the medium by a simple magnetic process. Noble metal nanoparticles, such as Ag and Au, strongly absorb light in the visible region due to coherent oscillations of the metal conduction band electrons in strong resonance with visible frequencies of light. This phenomenon is known as Surface Plasmon Resonance (SPR) and is highly dependent on NP size, shape, surface, and dielectric properties of the surrounding medium.

The recent literature showed that no more photodegradation studies were performed with Ag-Fe_3O_4 nanocomposite to photodegrade the oxytetracycline antibiotic and ibuprophene. Chang et al. observed that 99% of bactericidal effects from magnetically-controlled Ag/Fe_3O_4 Nanoparticles [26]. Similarly, Padmavathy et al. found high bactericidal yields (98%) with Ag-Fe_3O_4 nanoparticles [27]. Ag nanoparticles easily cover the nanoparticle surface with a layer of stable oxides to enhance the solar absorption spectrum with better photothermal properties. Fe_3O_4 in combination with Ag results in a significant increase in the plasmon absorption bandwidth and promotes photo conversion. To further improve the performance of nanoparticles in photothermal conversion systems, In the practical application, some important points should be considered when selecting a photocatalyst: superb photocatalytic activity and easy recovery for reuse. Traditional methods to remove the photocatalyst from water systems, including centrifugation and filtration, can lead to catalyst loss and energy consumption. Since magnetic materials can be conveniently and quickly gathered and recovered through applying external magnetic fields, the design and synthesis of new magnetic catalysts are drawing increasing interest. The reusability of photocatalysts prevents the environment from being contaminated with nanomaterials. Shan, et al. investigated the photodegradation of oxytetracycline with Ag_2O/Fe_3O_4 Magnetic photocatalyst and found low yields (82%) [25]. Padmavathy et al. found high bactericidal yields (98%) with Ag-Fe_3O_4 nanoparticles [27]. Hoang, et al. investigated Ag@Fe_3O_4 core-shell nanoparticles on the sensing performance [35]. Mahmoudi, et al. found efficient removal of oxytetracycline (89%) antibiotic from aqueous media using UV/g-C_3N_4/Fe_3O_4 photocatalytic process [36]. Zhang, et al. found 89% oxytetracycline yields with magnetic MOFs heterojunction photocatalyst [37]. Liu, et al. studied the Photocatalytic degradation of tetracycline with Fe_3O_4/g-C_3N_4/TiO_2 catalyst under visible light and found 89% photodegradation yields [38]. Li, et al. studied the photocatalytic degradation of oxytetracycline in aqueous solution by Fe_2O_3 – TiO_2 nanopowder. 87% removals was detected [39]. Pirsaheb, et al. studied photocatalytic degradation of ibuprofen by the CuS-Fe_3O_4/RGO catalyst with yields as high as 92% [40]. Abboud, et al. enhanced the removal of ibuprofen by heterogeneous Fe_3O_4-MnO_2 catalysts [41]. Shariati, et al. degrade the basic fuchsin dye by tetranary magnetic nanocomposite as a good photocatalyst for organic compound degradation [42].

As stated above although high bactericidal effects were found with Ag-Fe_3O_4 nanocomposite in aforementioned studies the Ibuprophene and oxytetracycline yields detected in this study were extremely higher than the recent studies

Conclusion

In this study, the photodegradation of ibuprophene and oxytetracycline present in raw pharmaceutical wastewater was performed by laboratory scale Ag-Fe_3O_4 nanocomposites.99% maximum ibuprophene photodegradation yield was obtained at pH = 7.0 while 99% maximum oxytetracycline photodegradation yield was observed at pH = 5.0 at optimized operational conditions such as 300 mg/l pollutant concentrations, 1 mg/l Ag-Fe_3O_4 nanocomposite dose, after 45 min photooxidation time at a sunlight power of 60 W/m2. The Ag-Fe_3O_4 nanocomposite can be used 120 times with the same photocatalytic yield as high as 99%. The yields decreased slightly to 98% after 140 times utilization for both

Citation: Sponza DT, Öztekin R (2024) Photoremoval of Ibuprophenin and Oxytetracycline and some microorganisms from a pharmaceutical wastewater via Ag-Fe_3O_4 nanocomposites. Forefronts Proteom Sci. 1(1): 011-023. DOI: https://dx.doi.org/10.17352/fps.000002

pollutants. Under these optimized conditions all the organisms found in the raw pharmaceutical industry wastewater were removed by 99% yields. The physicochemical analysis based on FESEM, TEM, and XRD results showed that the Ag-Fe_3O_4 nanocomposite surface area was 117.598 m^2/g where the Ag appears as spherical, shiny, and a uniform structure with certain void regions.

Acknowledgement

Experimental analyses in this study were performed at the Laboratories of the Canada Research Center, Ottawa, Canada. The authors would like to thank this body for providing financial support.

References

1. Anand U, Adelodun B, Cabreros C, Kumar P, Suresh S, Dey A, Ballesteros F, Bontempi E. Occurrence, transformation, bioaccumulation, risk and analysis of pharmaceutical and personal care products from wastewater: a review. Environ Chem Lett. 2022; 20(6):3883–3904.

2. Akash S, Sivaprakash B, Rajamohan N, Govarthanan M, Elakiya BT. Remediation of pharmaceutical pollutants using graphene-based materials - A review on operating conditions, mechanism and toxicology. Chemosphere. 2022 Nov; 306:135520. doi: 10.1016/j.chemosphere.2022.135520. Epub 2022 Jun 30. PMID: 35780979.

3. Akhil D, Lakshmi D, Senthil Kumar P, Vo D-VN, Kartik A (2021) Occurrence and removal of antibiotics from industrial wastewater. Environ Chem Lett 19(2):1477–1507.

4. Bastami TR, Ahmadpour A, Hekmatikar FA. Synthesis of Fe_3O_4/Bi_2WO_6 nanohybrid for the photocatalytic degradation of pharmaceutical ibuprofen under solar light. J Ind Eng Chem. 2017; 51:244–254.

5. Ali I, Peng C, Naz I, Khan ZM, Sultan M, Islam T, Abbasi IA. Phytogenic magnetic nanoparticles for wastewater treatment: a review. RSC Advances. 2017;7(64):40158-40178.

6. Azócar MI, Alarcón R, Castillo A, Blamey JM, Walter M, Paez M. Capping of silver nanoparticles by anti-inflammatory ligands: Antibacterial activity and superoxide anion generation. J Photochem Photobiol B. 2019 Apr; 193:100-108. doi: 10.1016/j.jphotobiol.2019.02.005. Epub 2019 Feb 22. PMID: 30826583.

7. Davoudi M, Ehrampoush MH, Vakili T, Absalan A, Asghar Ebrahimi A. Antibacterial effects of hydrogen peroxide and silver composition on selected pathogenic Enterobacteriaceae. Int J Environ Health Eng. 2012;1(1):23.

8. Ghaseminezhad SM, Shojaosadati SA. Evaluation of the antibacterial activity of Ag/Fe_3O_4 nanocomposites synthesized using starch. Carbohydr Polym. 2016 Jun 25; 144:454-63. doi: 10.1016/j.carbpol.2016.03.007. Epub 2016 Mar 5. PMID: 27083838.

9. Ghaseminezhad SM, Shojaosadati SA, Meyer RL. Ag/Fe_3O_4 nanocomposites penetrate and eradicate S. aureus biofilm in an in vitro chronic wound model. Colloids Surf B Biointerfaces. 2018 Mar 1; 163:192-200. doi: 10.1016/j.colsurfb.2017.12.035. Epub 2017 Dec 21. PMID: 29301116.

10. Liu CX, Qin L, Zhang C, Zeng G, Huang D, Cheng M, Xu P, Yi H, Huang D. Chitosan-wrapped gold nanoparticles for hydrogen-bonding recognition and colorimetric determination of the antibiotic kanamycin. Microchim Acta. 2017;184(7):2097-2105.

11. Li WH, Yuea XP, Guo CS, Lv JP, Liu SS, Zhang Y, Xu J. Synthesis and characterization of magnetically recyclable Ag nanoparticles immobilized on Fe_3O_4@C nanospheres with catalytic activity. Appl Surf Sci. 2015; 335:23-28.

12. Liu CH, Zhou ZD, Yu X, Lv BQ, Mao JF, Xiao D. Preparation and characterization of Fe_3O_4/Ag composite magnetic nanoparticles. Inorg Mater. 2008;44(3):291-295.

13. Park M, Seo S, Lee IS, Jung JH. Ultraefficient separation and sensing of mercury and methylmercury ions in drinking water by using aminonaphthalimide-functionalized Fe_3O_4@SiO_2 core/shell magnetic nanoparticles. Chem Commun (Camb). 2010 Jul 7;46(25):4478-80. doi: 10.1039/c002905j. Epub 2010 Apr 22. PMID: 20411197.

14. Petrov DA, Ivantsov RD, Zharkov SM, Velikanov DA, Molokeev MS, Lin CR, Tso CT, Hsu HS, Tseng YT, Lin ES, Edelman IS. Magnetic and magneto-optical properties of Fe_3O_4 nanoparticles modified with Ag. J Magn Magn Mater. 2020; 493:165692.

15. Abbasnia A, Zarei A, Yeganeh M, Sobhi HR, Gholami M, Esrafili A. Removal of tetracycline antibiotics by adsorption and photocatalytic-degradation processes in aqueous solutions using metal organic frameworks (MOFs): a systematic review. Inorg Chem Commun. 2022; 145:109959.

16. Abolhasani S, Ahmadpour A, Bastami TR, Yaqubzadeh A. Facile synthesis of mesoporous carbon aerogel for the removal of ibuprofen from aqueous solution by central composite experimental design (CCD). J Mol Liq. 2019; 281:261-268.

17. Ai T, Jiang X, Zhong Z, Li D, Dai S. Methanol-modified ultra-fine magnetic orange peel powder biochar as an effective adsorbent for removal of ibuprofen and sulfamethoxazole from water. Adsorp Sci Tech. 2020;38(7-8):304-321.

18. Akash S, Sivaprakash B, Rajamohan N, Govarthanan M, Elakiya BT. Remediation of pharmaceutical pollutants using graphene-based materials - A review on operating conditions, mechanism and toxicology. Chemosphere. 2022 Nov; 306:135520. doi: 10.1016/j.chemosphere.2022.135520. Epub 2022 Jun 30. PMID: 35780979.

19. Akhil D, Lakshmi D, Senthil Kumar P, Vo DVN, Kartik A. Occurrence and removal of antibiotics from industrial wastewater. Environ Chem Lett. 2021;19(2):1477-1507.

20. Santoyo Salazar J, Perez L, de Abril O, Phuoc LT, Ihiawakrim D, Vazquez M, Greneche JM, Begin-Colin S, Pourroy G. Magnetic iron oxide nanoparticles in 10-40 nm range: composition in terms of magnetite/maghemite ratio and effect on the magnetic properties. Chem Mater. 2011;23(6):1379-1386.

21. Sun L, Li Y, Sun M, Wang H, Xu S, Zhang C, Yang Q. Porphyrin-functionalized Fe3O4@SiO2 core/shell magnetic colorimetric material for detection, adsorption and removal of Hg2+ in aqueous solution. New J Chem. 2011; 35:2697-2704.

22. Tan P, Qin JX, Liu XQ, Yin XQ, Sun LB. Fabrication of magnetically responsive core–shell adsorbents for thiophene capture: AgNO3-functionalized Fe3O4@ mesoporous SiO2 microspheres. J Mater Chem A. 2014; 2:4698-4705.

23. Tran N, Mir A, Mallik D, Sinha A, Nayar S, Webster TJ. Bactericidal effect of iron oxide nanoparticles on Staphylococcus aureus. Int J Nanomedicine. 2010 Apr 15; 5:277-83. doi: 10.2147/ijn.s9220. PMID: 20463943; PMCID: PMC2865022.

24. Wang H, Zhang W, Zhao J, Xu L, Zhou C, Chang L, Wang L. Rapid decolorization of phenolic azo dyes by immobilized laccase with Fe_3O_4/SiO_2 nanoparticles as support. Ind Eng Chem Res. 2013; 52:4401-4407.

25. Shan C, Su Z, Liu Z, Xu R, Wen J, Hu G, Tang T, Fang Z, Jiang L, Li M. One-Step Synthesis of Ag_2O/Fe_3O_4 Magnetic Photocatalyst for Efficient Organic Pollutant Removal via Wide-Spectral-Response Photocatalysis-Fenton Coupling. Molecules. 2023 May 17;28(10):4155. doi: 10.3390/molecules28104155. PMID: 37241896; PMCID: PMC10222577.

26. Chang M, Lin WS, Xiao W, Chen YN. Antibacterial Effects of Magnetically-Controlled Ag/Fe_3O_4 Nanoparticles. Materials (Basel). 2018 Apr 24;11(5):659. doi: 10.3390/ma11050659. PMID: 29695121; PMCID: PMC5978036.

27. Padmavathy N, Chakraborty I, Kumar A, Roy A, Bose S, Chatterjee K. Fe3O4@ Ag and Ag@Fe3O4 Core–Shell Nanoparticles for Radiofrequency Shielding and Bactericidal Activity. Appl Nano Mater. 2022;5(1):237-248.

Citation: Sponza DT, Öztekin R (2024) Photoremoval of Ibuprophenin and Oxytetracycline and some microorganisms from a pharmaceutical wastewater via Ag-Fe_3O_4 nanocomposites. Forefronts Proteom Sci. 1(1): 011-023. DOI: https://dx.doi.org/10.17352/fps.000002

28. Hang BT, Anh TT. Controlled synthesis of various Fe_2O_3 morphologies as energy storage materials. Sci Rep. 2021 Mar 4;11(1):5185. doi: 10.1038/s41598-021-84755-z. PMID: 33664404; PMCID: PMC7933284.

29. Ahmadi M, Ramezani Motlagh H, Jaafarzadeh N, Mostoufi A, Saeedi R, Barzegar G, Jorfi S. Enhanced photocatalytic degradation of tetracycline and real pharmaceutical wastewater using MWCNT/TiO_2 nano-composite. J Environ Manage. 2017 Jan 15;186(Pt 1):55-63. doi: 10.1016/j.jenvman.2016.09.088. Epub 2016 Nov 13. PMID: 27852522.

30. Daghrir R, Drogui P. Tetracycline antibiotics in the environment: a review. Environ Chem Lett. 2013; 11:209-227.

31. Standard Methods for Water and Wastewater Examinations. USA. 2022; 300.

32. Degen P, Paulus M, Maas M, Kahner R, Schmacke S, Struth B, Tolan M, Rehage H. In situ observation of gamma-Fe_2O_3 nanoparticle adsorption under different monolayers at the air/water interface. Langmuir. 2008 Nov 18;24(22):12958-62. doi: 10.1021/la802394a. Epub 2008 Oct 14. PMID: 18850729.

33. Hunge YM, Yadav AA, Kang SW, Kim H. Photocatalytic degradation of tetracycline antibiotics using hydrothermally synthesized two-dimensional molybdenum disulfide/titanium dioxide composites. J Colloid Interface Sci. 2022 Jan 15;606(Pt 1):454-463. doi: 10.1016/j.jcis.2021.07.151. Epub 2021 Aug 2. PMID: 34399362.

34. Li R, Li Y, Wu J, Zhen Q. Photocatalytic degradation and pathway of oxytetracycline in aqueous solution by Fe_2O_3–TiO_2 nanopowder. RSC Advances. 2015;5(51):40764-40771.

35. Hoang VT, Tufa LT, Lee J, Doan MQ, Ha NH, Anh VT, Tran Le AT. Tunable SERS activity of Ag@Fe_3O_4 core-shell nanoparticles: Effect of shell thickness on the sensing performance. J Alloys Compd. 2023; 933:167649.

36. Mahmoudi K, Farzadkia M, Rezaei Kalantary R, Sobhi HR, Yeganeh M, Esrafili A. Efficient removal of oxytetracycline antibiotic from aqueous media using UV/g-C_3N_4/Fe_3O_4 photocatalytic process. Heliyon. 2024 May 1;10(9):e30604. doi: 10.1016/j.heliyon.2024.e30604. PMID: 38765134; PMCID: PMC11098847.

37. Zhang Z, Du C, Zhang Y, Yu G, Xiong Y, Zhou L, Liu Y, Chi T, Wang G, Su Y, Lv Y, Zhu H. Degradation of oxytetracycline by magnetic MOFs heterojunction photocatalyst with persulfate: high stability and wide range. Environ Sci Pollut Res Int. 2022 Apr;29(20):30019-30029. doi: 10.1007/s11356-021-17971-9. Epub 2022 Jan 8. PMID: 34997501.

38. Liu Y, Zheng X, Zhang S, Sun S. Enhanced removal of ibuprofen by heterogeneous photo-Fenton-like process over sludge-based Fe_3O_4-MnO_2 catalysts. Water Sci Technol. 2022 Jan;85(1):291-304. doi: 10.2166/wst.2021.612. PMID: 35050884.

39. Li R, Zhang X, Han Sun Y, Jin Liu RJ. Photocatalytic degradation of tetracycline with Fe_3O_4/g-C_3N_4/TiO_2 catalyst under visible light. Carbon Lett. 2024.

40. Pirsaheb M, Hossaini H, Fatahi N, Jafari Z, Jafari F, Motlagh Jafari R. The visible-light photocatalytic degradation of ibuprofen by the CuS-Fe_3O_4/RGO catalyst. Inorg Chem Commun. 2023;111597.

41. Abboud M, Youssef S, Podlecki J, Habchi R, Germanos G, Foucaran A. Superparamagnetic Fe_3O_4 nanoparticles, synthesis and surface modification. Mater Sci Semicond Process. 2015; 39:641-648.

42. Shariati M, Babaei A, Azizi A. Synthesis of the tetranary magnetic nanocomposite as a good photocatalyst for degradation of basic fuchsin dye in aqueous media under visible light: Characterization, response surface methodology, and kinetic study. J Mater Res. 2023; 38:2666-2678.

Citation: Sponza DT, Öztekin R (2024) Photoremoval of Ibuprophenin and Oxytetracycline and some microorganisms from a pharmaceutical wastewater via Ag-Fe_3O_4 nanocomposites. Forefronts Proteom Sci. 1(1): 011-023. DOI: https://dx.doi.org/10.17352/fps.000002